Supplementary Information

MRI Acquisition

MRI scans were conducted at the New York State Psychiatric Institute using sequences adapted from the Human Connectome Project (HCP; http://protocols.humanconnectome.org/HCP/3T/imaging-protocols.html) for a GE Signa 3T MR750 scanner (Milwaukee, WI) with a standard 32-channel Nova head coil. A 3-plane spin-echo localizing scan was used to position the axial functional images parallel to the anterior commissure-posterior commissure line. Each participant completed two high-resolution T1-weighted BRAVO structural scans (flip angle = 12°, field of view = 24x24cm, 0.8mm isotropic voxels) and a high-resolution T2-weighted scan (TR = 2500ms, TE = max, field of view = 25.6x25.6cm, 0.8mm isotropic voxels). Prior to the functional scans, two short spin-echo, echo-planar imaging (EPI) sequences (TR=5200ms, TE=25ms, field of view=19.2x19.2cm, 2mm isotropic voxels, 72 slices with no gaps) were acquired with opposite phase encoding (anterior-posterior vs. posterior-anterior) to measure the B0 field for EPI distortion correction. Two runs of eyes-open resting state functional data were acquired using a T2*-weighted multi-band EPI pulse sequence (TR = 850ms, TE = 25ms, flip angle = 60°, multi-band factor = 6, field of view = 19.2x19.2cm, 2 mm isotropic voxels, 66 slices with no gaps, 7min 32s = 532 frames per run).

MRI Processing

The pre- and post-processing and analysis of MRI data are summarized in Figure S1. Twelve frames of scanner calibration data were reconstructed as two volumes and discarded prior to preprocessing. Data were preprocessed using the HCP "minimal preprocessing" pipelines v3.4 (1). After preprocessing, six additional frames from the beginning of each functional run were removed to account for the scanner reaching steady state. First-level analyses were performed in "grayordinate" space ("91k" CIFTI format: 91,282 grayordinates comprising 32,492 per cortical hemisphere and 29,298 subcortical), which combines cortical surface and subcortical volume representations. CIFTI format data were converted into a temporary NIFTI format that is readable by commonly used programs that are not currently compatible with CIFTI format using the HCP Workbench software (*wb_command -cifti-convert -to-nifti*).

Additional processing was performed in Matlab R2019a (Mathworks, 2019). Using commands from Analysis of Functional NeuroImages v19.2.24 (AFNI; http://afni.nimh.nih.gov/) and FMRIB Software Library v6.0.1 (FSL; http://fsl.fmrib.ox.ac.uk/fsl/fslwiki/) software, BOLD signal was demeaned and detrended (AFNI 3dDetrend), despiked (AFNI 3dDespike -localedit), and bandpass filtered (FSL fslmaths 0.01-0.08 Hz).

Statistical Analysis using Network Based Statistic (NBS)

We parcellated the brain (*wb_command -cifti-parcellate*) based on a previously defined atlas (https://balsa.wustl.edu/file/show/JX5V), which defined 333 cortical regions based on homogeneity of resting state functional connectivity (2) and 19 anatomically defined subcortical regions from the FreeSurfer Subcortical Atlas (left and right amygdala, hippocampus, accumbens, caudate, pallidum, putamen, thalamus, ventral

diencephalon, cerebellum, and brainstem). The resulting 352 parcels were used as "nodes" for NBS analysis. The average timecourse from each parcel was extracted and correlated with timeseries from every other parcel, generating a 352x352 correlation matrix for each participant. These participant-level correlation matrices were used as inputs into the NBS Connectome v1.2 software.

The NBS procedure consisted of several steps. First, a general linear model was calculated to test for group differences in each unique cell (region-to-region functional connectivity, "edges") in the 352x352 matrices, controlling for age, sex, and residual head motion (mean FD). Next, an initial statistical threshold was set (here, $f>14$ for the group difference effect) and components/clusters of supra-threshold edges were identified, i.e. sets of edges sharing start/end nodes. Random permutations (n=10,000) were computed by shuffling group membership to generate a null distribution of maximum component size (number of edges or "extent") identified using same the procedure as above. Finally, the p-values of identified components in the unpermuted dataset were determined from this null distribution based on their extent and components passing $p<.05$ were extracted. This approach has been shown to improve power relative to FDR correction as the number of regions and connections analyzed increases as well as with increasing component sizes.

Results from NBS can differ based on the selection of the initial edge-wise threshold (here, the f-statistic) or based on whether the components are measured by extent as described above or, alternately, by "intensity," calculated as the sum of test statistic values across all edges in the component. To ensure that our results were not due to an artifact of the NBS parameters we initially selected, we replicated our analyses using various f-thresholds ($f = 13$, 14, or 15) and both extent and intensity component measurements (Table S1). As expected, using a more stringent (higher) f-statistic threshold resulted in a single significant component with fewer edges, while a lower f-threshold yielded a single significant component with more edges. At each edge-wise threshold, extent and intensity thresholding yielded the same significant component. The identified edges in these components calculated with different NBS parameters overlapped with those reported in the main text, and the component retained its overall structure with a "hub" in the medial temporal gyrus.

Reconstruction Independent Components Analysis (RICA)

We used Reconstruction Independent Components Analysis (RICA) to isolate distinct independent (sub)components (IC) within the NBS results. RICA was performed in Matlab R2019a (Mathworks, 2019) using the function 'rica' (https://www.mathworks.com/help/stats/rica.html). Briefly, the RICA algorithm maps the input data (i.e., each participant's connectivity at each of the 23 individual edges) to output ICs by assigning weights or "loadings" to each individual edge. For each participant, a value for each IC was calculated as a weighted average across all edges, weighted by their RICA loadings.

NBS Using Schaefer Parcellation

To test robustness of our NBS analyses, we conducted a sensitivity analysis aimed to replicate findings using a coarser 100 parcel segmentation (3). This segmentation created parcels based on a gradient-weighted Markov Random Field model, which

defines parcel borders accounting for both abrupt local changes in functional connectivity (a putative proxy for histological or visuotopic functional MRI boundaries) and global homogeneity in resting state functional connectivity. The timeseries of activity from each of the 100 parcels ("nodes") was extracted and correlated with all other nodes, resulting in 10,000 connections ("edges") of which 4,950 were unique, non-diagonal elements. These correlations were Fisher r-to-z transformed, resulting in a 100x100 connectivity matrix for each participant, which were analyzed using NBS.

NBS revealed one component with significantly altered connectivity in patients relative to controls ($p = .017$). This component consisted of 6 edges, all connecting a single node ("hub") in the right middle temporal lobe to nodes in the salience/ventral attention (SAL/VAN) and somatomotor networks (Table S2, Figure S2). These edges all showed reduced connectivity in OCD relative to HC participants, with 5 out of 6 edges showing negative connectivity in OCD and positive or close to zero connectivity in HC.

Unlike the NBS analyses presented in the main text, the edges in the identified NBS component from the Schaefer parcellation were relatively homogenous in their overall rs-FC (positive vs. negative on average) and completely homogenous in the direction of group difference (all OCD<HC). Therefore, we had no reason to conduct RICA to subdivide this component to resolve heterogeneity.

Group Differences Analysis Using Mass Univariate Approach

The NBS technique has increased power compared to mass univariate approaches (e.g., FDR correction for testing multiple edges individually) to identify components (i.e., sets of overlapping edges) that are significant in the aggregate. Importantly, the individual edges are not intended to, and cannot, be interpreted in isolation from the component (Zalesky et al., 2010). Therefore, in order to evaluate whether any edges individually predicted treatment response, as in prior work (Cyr et al., 2020) we performed an FDR-corrected mass univariate test as implemented in the NBS Connectome v1.2 software and tested for treatment response prediction in the edges that overlapped between the NBS and mass univariate methods.

Using the Gordon parcellation, the mass univariate approach identified 7 edges that statistically significantly differed between OCD and HC after FDR correction, 3 of which were included in the component identified by NBS (Table S3). Analogously to the LME analyses performed in the main text, we fit LME models to assess treatment response prediction in each of these 3 edges. None of the edges were significant predictors of treatment response.

With the Schaefer parcellation, the mass univariate approach identified 2 edges that differed significantly between OCD and HC after FDR correction, neither of which were included in the component identified by NBS (Table S4). Because neither of these edges overlapped with the component identified by NBS, we did not test treatment prediction on these edges.

References

1. M. F. Glasser *et al.*, The minimal preprocessing pipelines for the Human Connectome Project. *Neuroimage* **80**, 105-124 (2013).
2. E. M. Gordon *et al.*, Generation and Evaluation of a Cortical Area Parcellation from Resting-State Correlations. *Cereb Cortex* **26**, 288-303 (2016).
3. A. Schaefer *et al.*, Local-Global Parcellation of the Human Cerebral Cortex from Intrinsic Functional Connectivity MRI. *Cereb Cortex* **28**, 3095-3114 (2018).

Figure S1. Pre-processing, post-processing, and analysis pipeline used for resting state functional MRI data.

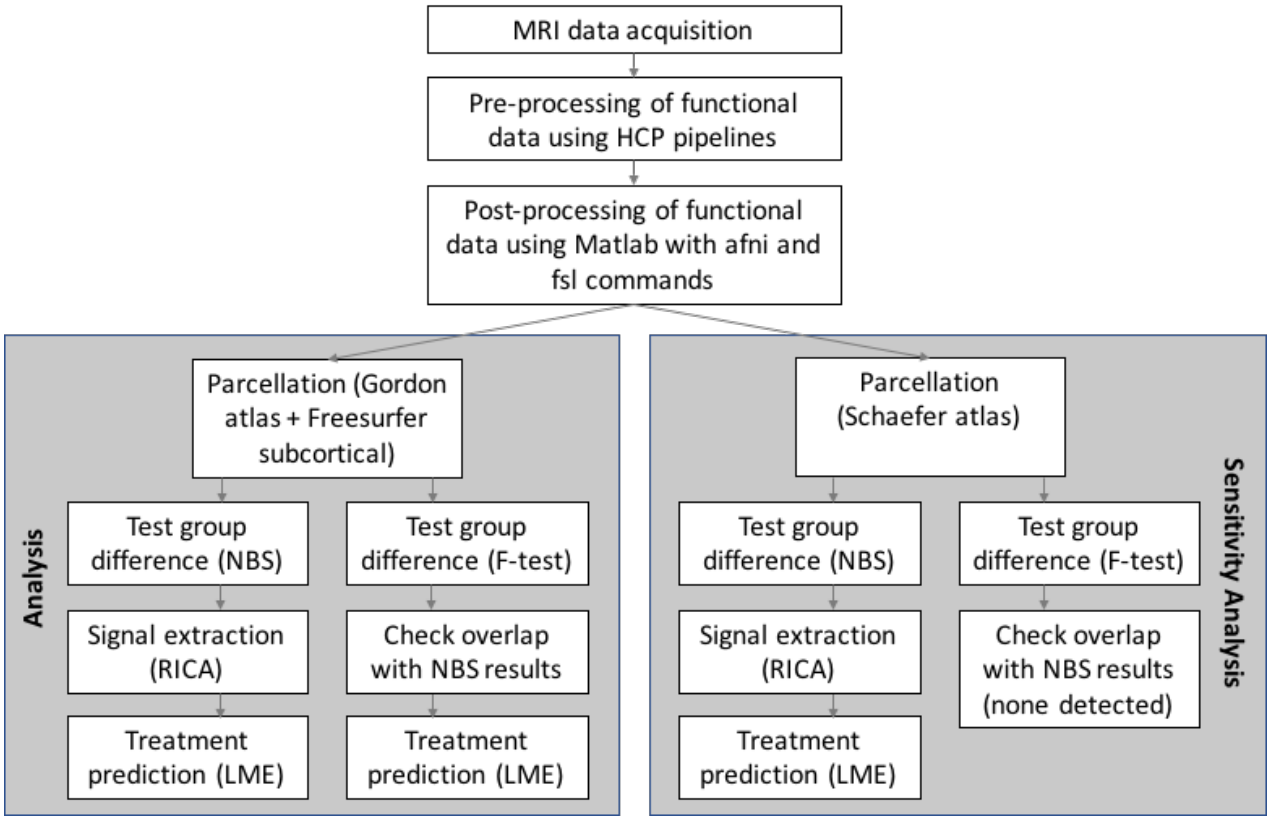

Table S1. Edges with significant group differences for different NBS parameters.

Edge		Included in significant component from NBS?**		
Node 1*	**Node 2***	**F > 13**	**F > 14 (used in main analyses)**	**F > 15**
R_VentralAttn_12	L_CinguloOperc_10	X	**X**	X
R_VentralAttn_12	R_CinguloOperc_33	X	**X**	X
R_VentralAttn_12	L_CinguloOperc_11	X		
R_VentralAttn_12	R_CinguloOperc_34	X		
R_VentralAttn_12	L_Auditory_10	X	**X**	
R_VentralAttn_12	R_Auditory_22	X	**X**	
R_VentralAttn_13	L_Default_7	X	**X**	X
R_VentralAttn_13	R_Default_27	X	**X**	X
R_VentralAttn_13	L_CinguloOperc_2	X	**X**	X
R_VentralAttn_13	L_CinguloOperc_10	X	**X**	X
R_VentralAttn_13	L_CinguloOperc_13	X	**X**	X
R_VentralAttn_13	R_CinguloOperc_33	X	**X**	X
R_VentralAttn_13	R_CinguloOperc_37	X	**X**	X
R_VentralAttn_13	R_CinguloOperc_38	X	**X**	X
R_VentralAttn_13	R_CinguloOperc_27	X	**X**	
R_VentralAttn_13	R_CinguloOperc_30	X	**X**	
R_VentralAttn_13	L_CinguloOperc_1	X		
R_VentralAttn_13	L_MedialParietal_3	X	**X**	X
R_VentralAttn_13	R_Visual_38	X	**X**	X
R_VentralAttn_13	L_SMmouth_2	X	**X**	X
R_VentralAttn_13	R_SMmouth_6	X	**X**	X
R_VentralAttn_13	R_Auditory_19	X		
R_VentralAttn_13	R_Auditory_22	X		
R_VentralAttn_16	L_CinguloOperc_16	X	**X**	
R_VentralAttn_16	R_CinguloOperc_30	X	**X**	
R_VentralAttn_16	R_CinguloOperc_34	X	**X**	
R_VentralAttn_16	L_CinguloOperc_1	X		
R_VentralAttn_16	L_CinguloOperc_10	X		
R_VentralAttn_16	L_Auditory_2	X		
L_DorsalAttn_17	L_CinguloOperc_2	X	**X**	
L_CinguloOperc_10	L_None_18	X	**X**	X
L_ParietoOccip_1	L_SMmouth_4	X		
R_ParietoOccip_5	L_SMmouth_4	X		
L_ParietoOccip_1	L_Putamen	X		
L_ParietoOccip_2	L_Putamen	X		
R_ParietoOccip_5	L_Putamen	X		
R_Default_21	L_Putamen	X		
R_Auditory_19	L_Putamen	X		
Component summary				
Number of edges in component		38	23	15
Component p-value (extent thresholding)		.031	.027	.022
Component p-value (intensity thresholding)		.022	.044	.040

* All edges are undirected. The numberings as node 1 and 2 are arbitrary.
** At each edge-wise (f-statistic) threshold, extent and intensity thresholding yielded the same significant component.

Table S2. Resting state functional connectivity group differences (alternate parcellation).

Parcel 1*			Parcel 2*			Mean edge values	
Parcel Name	**Description**	**Center (MNI)**	**Parcel Name**	**Description**	**Center (MNI)**	**OCD**	**Controls**
17Networks_RH_ TempPar_2	Superior temporal gyrus	57 -26 -2	17Networks_LH_SalVentAttnA_ ParOper_1	Inferior parietal lobule	-59 -38 29	-0.14	0.11
17Networks_RH_ TempPar_2	Superior temporal gyrus	57 -26 -2	17Networks_LH_SalVentAttnA_ Ins_2	Insula	-38 12 6	-0.21	0.02
17Networks_RH_ TempPar_2	Superior temporal gyrus	57 -26 -2	17Networks_LH_SalVentAttnA_ ParMed_1	Cingulate gyrus	-11 -34 45	-0.23	0.00
17Networks_RH_ TempPar_2	Superior temporal gyrus	57 -26 -2	17Networks_RH_SalVentAttnA_ ParOper_1	Inferior parietal lobule	61 -26 27	-0.08	0.15
17Networks_RH_ TempPar_2	Superior temporal gyrus	57 -26 -2	17Networks_RH_SomMotA_3	Postcentral gyrus	30 -37 64	-0.04	0.17
17Networks_RH_ TempPar_2	Superior temporal gyrus	57 -26 -2	17Networks_RH_SomMotB_S2_2	Precentral gyrus	57 -4 11	0.07	0.29

This table details the 6 edges that comprised the NBS component with a significant group difference between patients with OCD and healthy controls for the alternate parcellation reported in the Supplemental text (also shown in Figure S2). Edges are identified by the nodes (parcels) they connect. Parcel names are those used by the parcellation authors (Schaefer et al., 2018). Center (MNI) values are the coordinates of the center of mass for each parcel. Parcel descriptions are assigned using the Talairach Daemon (http://talairach.org/daemon.html).

* Note: all edges are undirected. Parcels are numbered as 1 and 2 simply for reference; this does not indicate directionality of the connection.

Figure S2. Resting state functional connectivity group differences (alternate parcellation). Visualization of the 6 edges comprising the NBS component that differed significantly across patients with OCD and healthy controls with the alternate parcellation described in the Supplement (details in Table S2). Nodes (endpoints of edges) are plotted by center of mass. All 6 edges (21) had greater average connectivity in healthy controls (HC) compared to the OCD group.

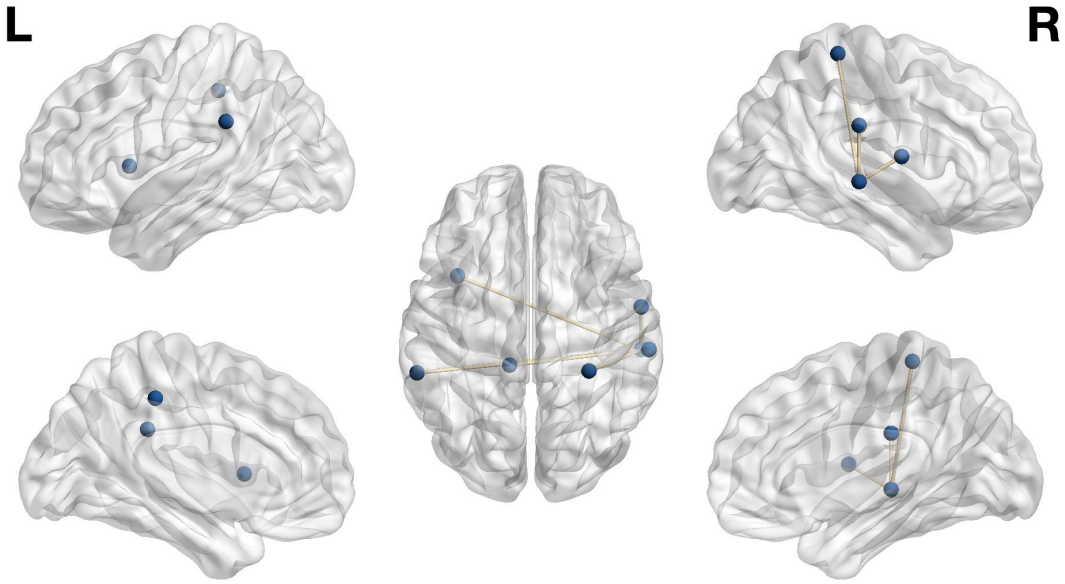

Table S3. Resting state functional connectivity group differences (mass univariate approach) using the Gordon parcellation.

Parcel 1*			Parcel 2*			Mean edge values	
Parcel Name	**Description**	**Center (MNI)**	**Parcel Name**	**Description**	**Center (MNI)**	**OCD**	**Controls**
R_VentralAttn_13	**Middle temporal gyrus**	**57.2 -34.2 -2.4**	**L_CinguloOperc_10**	**Insula**	**-38.0 6.3 10.1**	**-0.28**	**0.00**
R_VentralAttn_13	**Middle temporal gyrus**	**57.2 -34.2 -2.4**	**R_CinguloOperc_33**	**Insula**	**37.4 4.7 13.0**	**-0.26**	**-0.01**
R_VentralAttn_13	**Middle temporal gyrus**	**57.2 -34.2 -2.4**	**R_Visual_38**	**Cuneus**	**6.5 -77.8 28.4**	**-0.26**	**-0.03**
R_Visual_39	Cuneus	14.5 -70.2 22.0	L_None_21	Superior Temporal Gyrus	-51.1 7.0 -18.0	-0.18	0.08
L_Pallidum	Lentiform Nucleus	-21.3 -2.4 -0.1	L_SMhand_8	Medial Frontal Gyrus	-5.0 -15.1 51.3	0.04	-0.12
L_Putamen	Lentiform Nucleus	-28.0 2.0 1.0	L_ParietoOccip_2	Parahippocampal Gyrus	-10.7 -50.9 5.4	-0.20	0.00
L_Putamen	Lentiform Nucleus	-28.0 2.0 1.0	R_Auditory_19	Insula	39.1 -14.8 19.4	0.14	-0.05

This table details the 7 edges that were identified as significantly different between OCD and HC after FDR-correction of a mass univariate approach (i.e., F-test) testing all edges in the Gordon parcellation. Edges are identified by the nodes (parcels) they connect. Parcel names are those used by the BALSA database (https://balsa.wustl.edu/file/show/JX5V). Center (MNI) values are the coordinates of the center of mass for each parcel. Parcel descriptions are assigned using the Talairach Daemon (http://talairach.org/daemon.html). **Bold** indicates edges that were also included in the significant NBS component (Table 2).
* Note: all edges are undirected. Parcels are numbered as 1 and 2 simply for reference; this does not indicate directionality of the connection.

Table S4. Resting state functional connectivity group differences (mass univariate approach) using the Schaefer parcellation.

Parcel 1*			Parcel 2*			Mean edge values	
Parcel Name	**Description**	**Center (MNI)**	**Parcel Name**	**Description**	**Center (MNI)**	**OCD**	**Controls**
17Networks_LH_TempPar_1	Superior temporal gyrus	-57 -50 12	17Networks_RH_ DorsAttnA_TempOcc_1	Middle occipital gyrus	49 -60 -11	-0.03	0.21
17Networks_RH_ContA_IPS_1	Inferior parietal lobule	38 -45 49	17Networks_RH_ VisCent_ExStr_3	Middle temporal gyrus	36 -82 16	0.30	0.03

This table details the 2 edges that were identified as significantly different between OCD and HC after FDR-correction of a mass univariate approach (i.e., F-test) testing all edges in the Schaefer parcellation. Neither of these edges overlapped with the significant NBS component. Edges are identified by the nodes (parcels) they connect. Parcel names are those used by the parcellation authors (Schaefer et al., 2018). Center (MNI) values are the coordinates of the center of mass for each parcel. Parcel descriptions are assigned using the Talairach Daemon (http://talairach.org/daemon.html).

* Note: all edges are undirected. Parcels are numbered as 1 and 2 simply for reference; this does not indicate directionality of the connection.